Available online at www.sciencedirect.com

SciVerse ScienceDirect

Journal of Nutritional Biochemistry 23 (2012) 169–178

Journal of Nutritional Biochemistry

Redox homeostasis and posttranslational modifications/activity of phosphatase and tensin homolog in hepatocytes from rats with diet-induced hepatosteatosis☆

Anna Alisi[a,*], Giovannella Bruscalupi[b], Anna Pastore[c], Stefania Petrini[d], Nadia Panera[a], Mara Massimi[e], Giulia Tozzi[f], Silvia Leoni[b], Fiorella Piemonte[f,1], Valerio Nobili[a,1]

[a]Unit of Metabolic and Autoimmune Liver Diseases of Bambino Gesù Children's Hospital-IRCCS, Rome, Italy
[b]Department of Biology and Biotechnology "C. Darwin", "La Sapienza" University, P.le Aldo Moro 5; 00185 Rome, Italy
[c]Laboratory of Biochemistry of Bambino Gesù Children's Hospital-IRCCS, Rome, Italy
[d]Microscopy Unit, of Bambino Gesù Children's Hospital-IRCCS, Rome, Italy
[e]Department of Basic and Applied Biology, University of L'Aquila, L'Aquila, Italy
[f]Neuromuscular and Neurodegenerative Diseases Unit, of Bambino Gesù Children's Hospital-IRCCS, Rome, Italy

Received 28 June 2010; received in revised form 9 November 2010; accepted 16 November 2010

Abstract

High-fat and high-carbohydrate diets may predispose to simple steatosis, alone or associated with necroinflammation and fibrosis (steatohepatitis). However, there are few reports about the real effect of these nutrients on hepatocyte redox homeostasis and consequent molecular derangement. Here, we investigated whether different diets would induce oxidative damage in primary rat hepatocytes and thereby affect the activity of phosphatase and tensin homolog (PTEN).

We used Sprague–Dawley rats fed, for 14 weeks, a standard diet (SD), a high-fat/low-carbohydrate diet (HFD-LC), a normal-fat/high-fructose diet (NFD-HF), or a high-fat/high-fructose diet (HFD-HF). Metabolic and histological parameters were analyzed in blood and liver samples, while oxidative stress markers and related posttranscriptional modification of PTEN were analyzed in isolated hepatocytes.

Our results indicate that different dietetic hypercaloric regimens caused liver damage and a significant increase of body and liver weight, as well as elevated plasma levels of alanine aminotransferase, triglycerides and insulin. Hepatocytes from NFD-HF and HFD-HF rats displayed a decrement of cell viability and proliferation rate. Hepatocytes from animals treated with hypercaloric regimens also exhibited oxidative stress greater than SD hepatocytes. Finally, NFD-HF and HFD-HF hepatocytes showed an increased PTEN phosphorylation and decreased PTEN activity, which seem strongly correlated to an increased glutathionylation of the protein.

In conclusion, we demonstrate that fructose-enriched diets cause a tissue and hepatocyte damage that might exacerbate those observed in the presence of high-fat alone and might render, via redox homeostasis imbalance, the hepatocytes more prone to posttranslational modifications and activity alteration of PTEN.

Keywords: Hepatocytes; Hepatosteatosis; Glutathione; Oxidative stress; PTEN

1. Introduction

Energy balance in the body is controlled by a number of overlapping systems influencing both caloric intake and energy expenditure. It is well known that consumption both of a high-fat diet and/or high-fructose diet may alter the homeostatic regulation of energy balance and cause obesity as well as some features of metabolic syndrome [1–4]. Obesity, diabetes and associated medical conditions have been increasing over the years, concomitantly with increased availability and consumption of hypercaloric and more palatable foods (i.e., snack foods and fast food meals) [5–7].

High-fat diet consumption has been shown to induce weight gain, insulin resistance and hyperlipidemia in humans and animals [8–12]. Recently, it has also been reported that long-term consumption of a high-fat diet during pregnancy enhances susceptibility of the progeny to developing a metabolic syndrome-like phenotype in adult life in mice [13]. Diets with a high glycemic index and glycemic load are positively associated with insulin resistance, and intake of refined carbohydrates is also associated with insulin resistance [14–16]. In particular, a high-fructose diet is able to induce insulin resistance, hypertension and dyslipidemia in animal models of metabolic syndrome, suggesting that excessive fructose intake would have a similar negative influence on human health [17–19]. Stanhope et al.

☆ Funding: The study was entirely supported by Bambino Gesù Children's Hospital and Research Institute, Rome, Italy.

* Corresponding author. Unit of Metabolic and Autoimmune Liver Diseases of "Bambino Gesù" Children's Hospital and Research Institute, Piazzale S. Onofrio 4, 00165 Rome, Italy. Tel.: +39 06 68592650; fax: +39 06 68592904.

E-mail address: anna.alisi@opbg.net (A. Alisi).

[1] These authors have contributed equally to this study.

0955-2863/$ - see front matter © 2012 Elsevier Inc. All rights reserved.
doi:10.1016/j.jnutbio.2010.11.013

demonstrated that the dietary fructose increases *de novo* lipogenesis and visceral adiposity, promotes dyslipidemia and decreases insulin sensitivity in overweight/obese subjects [20]. A recent work demonstrated that daily fructose ingestion is associated with a reduced hepatic steatosis but increased fibrosis in patients with nonalcoholic fatty liver disease (NAFLD) [21].

Interestingly, several studies have demonstrated that nutritional models, including the use of a fructose-rich and fat-rich diet, may also induce alterations of liver cell homeostasis, causing predisposition to NAFLD [22–24]. NAFLD is a liver disorder with multiple features, including fatty infiltration in the liver alone (simple steatosis) or associated with necroinflammation and fibrosis (steatohepatitis, or NASH) [25,26]. Genetic background and lifestyle factors are considered the major contributors to the pathogenesis of NAFLD/NASH both in children and adults [27,28]. However, even though both nutrition and physical activity are major factors in determining its manifestation, the exact chain of causative events and molecular mechanisms involved in the pathogenesis of NAFLD/NASH still remains unclear. To this aim, several rodent models have been developed, but actually, the development of steatosis and steatohepatitis due to overfeeding represents the best model to mimic human NAFLD/NASH. However, the real effects of an excessive caloric intake diet may be strictly dependent on the rodent strain. In fact, the administration of a high-fat diet to Wistar rats for up to 14 weeks caused few metabolic alterations and no abnormalities in liver histology [29], while Sprague–Dawley rats fed both a liquid or solid high-fat diet seem more susceptible to developing NAFLD/NASH [30,31]. However, often these diets are fat-rich but carbohydrate-poor, so a normal carbohydrate content is restored by administration of sugars in animal drinking water [32]. Moreover, interestingly, a "cafeteria diet" high in processed sugars and fat is able to promote the development of hepatic steatosis in nonobese rats [33].

Several of these models demonstrated that oxidative stress may solve part of the mystery around pathogenesis of NAFLD/NASH, and it might explain most of the second-level events resulting in the appearance of steatohepatitis [34,35]. Moreover, oxidative stress, which is a consequence of an imbalance between pro-oxidants and antioxidants, has been thought to play a role in diet-induced liver impairment [34,36]. High-fat diets increase hepatic reactive oxygen and nitrogen species, which, in turn, induce mitochondrial dysfunction, hypoxic stress and increased substrates available for oxidation (i.e., proteins) [37]. Lipid and protein oxidation products were also higher in high-fat high-sucrose diet-fed rats [38]. On the other hand, an impaired glutathione (GSH) metabolism, in the direction of an oxidant status, correlates with a higher intake of saturated fat and a lower intake of carbohydrates in NASH subjects [39].

All these findings have been derived mostly from the study of plasma or tissue markers of oxidative stress, while there are few reports about the real effects of diet on hepatocyte homeostasis.

Here, we study cellular and redox homeostasis of primary hepatocytes isolated from rats fed with a high-fructose diet and/or high-fat diet.

Furthermore, since we have recently demonstrated that protein glutathionylation largely increases in a pediatric model of NAFLD/NASH, we also investigated the role of oxidative stress and GSH in regulating the activity of phosphatase and tensin homolog (PTEN), which is emerging as an important player in the pathogenesis of NAFLD [40,41].

2. Materials and methods

2.1. Animals

Forty male Sprague–Dawley rats (120–140 g) were obtained from Harlan Italy (San Pietro al Natisone, UD, Italy). All animals received proper care and treatment in agreement with the guidelines of the local committee. They were housed in plastic cages under standard conditions with free access to water and food. The cages were maintained in a clean independent rack at the Certified Animal Facility of the University of Rome, "La Sapienza." After being fed with standard rat chow for 5 days, the animals were equally divided into four different groups (10 rats/group) based on dietetic regimen: a standard diet (SD), a high-fat/low-carbohydrate diet (HFD-LC), a normal-fat/high-fructose (NFD-HF) diet, or a high-fat/high-fructose diet (HFD-HF).

Normal SD contained 5% of energy derived from fat, 18% from proteins, and 77% from carbohydrates (3.3 kcal/g), while high-fat diet contained 58% of energy derived from fat, 18% from protein, and 24% from carbohydrates (5.6 kcal/g; Laboratorio Dottori Piccioni, Gessate Milano, Italy). Fructose (30%) was added to the drinking water.

The experiment was terminated after 14 weeks, at the end of which the animals were subjected to fasting for approximately 8 h, with free access to simple water, before to be used for next experiments. In detail, randomly six animals from each group were used to obtain blood samples for biochemistry and liver tissue for histology and later molecular studies, while four from each group were used to isolate primary hepatocytes using a perfusive method (see below).

2.1.1. Biochemical determinations

Blood obtained from portal vein by aspiration methods before liver removal in anesthetized animals was collected in sterile glass tubes containing 0.15% ethylenediaminetetraacetic acid. Blood was used to obtain plasma after 3,000 rpm centrifugation at 4°C for 15 min. Plasma samples were immediately used to perform enzymatic and photocolorimetric assay to determine the levels of alanine aminotransferase (ALT), triglycerides, total cholesterol, glucose and insulin. Enzymatic and colorimetric assays were performed using standard procedures as indicated by kits purchased from different companies: ALT assay kit from Randox Laboratories Ltd. (Antrim, UK), triglycerides and cholesterol assay kits from Cayman Chemical (Ann Arbor, MI, USA), glucose assay kit from Abcam Inc. (Cambridge, MA, USA), and rat insulin enzyme immunoassay kit from SPI-BIO (France).

At 14 weeks, insulin resistance was calculated according to the homeostasis model assessment of insulin resistance (HOMA-IR) calculation: fasting plasma insulin (μU/ml)×fasting plasma glucose (mmol/l)/22.5.

Frozen liver tissue (100 mg) was homogenized in chloroform/methanol solution (2:1). The solution was vortexed and filtered. After adding 0.1 ml of 0.58% NaCl solution, the filtrate was centrifuged at 1,000 rpm for 5 min. The upper phase was aspirated, while the chloroform phase was analyzed by using Triglyceride Reagent (Sigma Diagnostics, St. Louis, MO, USA). After a 10-min incubation at 30°C, the samples were read at 540 nm.

2.2. Liver histology and immunohistochemistry

The liver tissues were fixed in 40 g/l formaldehyde, embedded in paraffin. The liver tissue sections were stained with hematoxylin and eosin (H&E) and Masson's trichrome. Frozen sections of formalin-fixed liver (5 μm thick) were stained with Oil Red O. Each section was assessed under 10×40 light microscopic fields.

Immunohistochemistry for the evaluation of inflammatory infiltrate was carried out by using mouse anti-CD45 and mouse anti-CD163 (Dako Corp., Carpinteria, CA, USA). Detection of the primary antibody was carried out by using the appropriate secondary biotinylated antibody (Vector Laboratories, Bridgeport, NJ, USA) and the peroxidase DAB kit (Dako). To perform quantification of inflammatory infiltrate, CD45- and CD163-positive cells were counted (400-fold magnification) in at least 10 fields for each liver section (four of each group of treatment), and the mean value per field was calculated.

2.3. Isolation and culture of primary hepatocytes

Primary hepatocytes were isolated by collagenase perfusion, as already described [42]. Briefly, the rats were anesthetized by intraperitoneal administration of sodium pentobarbital (5 mg/100 g body weight). Perfusion of the livers was performed initially with a calcium-free Hank's balanced salt solution containing 2% bovine serum albumin and 0.6 mM ethyleneglycotetraacetic acid, and subsequently with Hank's solution containing 4 mM calcium chloride and 0.04 % collagenase, in a recirculating system at 37°C. The liver cells were released into a Krebs–Henseleit buffer with 2% bovine serum albumin by gentle dispersion of the tissue, resuspended and filtered. After three sequential centrifugations in RPMI 1640 medium plus 10% FBS, cell viability was determined by the Trypan blue dye exclusion method.

Some of the hepatocytes were collected and used to perform analysis of oxidative stress parameters, immunoprecipitation and Western blotting.

The remaining hepatocytes were seeded on collagen-coated plates at densities between 1.5×10^4 and 3×10^4 cells/cm^2. After a 60-min incubation at 37°C in an atmosphere of 5% CO_2–95% air, the medium was replaced by fresh medium. After 24 h from seeding, cell cytomorphology was examined by phase-contrast microscope, and cell homeostasis (cell viability and proliferation rate) was evaluated.

2.4. Cell viability and DNA synthesis

Cell viability was determined by neutral red assay based on the protocol described by Babich and Borenfreund [43]. This method determines cell viability by the evaluation of accumulation of the neutral red dye in the lysosomes of viable,

uninjured cells. Neutral red (Sigma, Italy) was dissolved in culture medium and added to cells for 1 h. The pH of the neutral red solution was adjusted in all the experiments to 6.35 with the addition of KH_2PO_4 (1 M). Cells were then washed with phosphate-buffered saline, and 1 ml of elution medium (EtOH/AcCOOH, 50%/1%) was added followed by gentle shaking for 10 min so that complete dissolution was achieved. Spectrophotometer measurement was performed at 540-nm absorbance.

Thymidine incorporation was evaluated after a 2-h incubation with thymidine according to the already described protocol [44]. The resulting data were used to measure the rate of DNA synthesis.

2.5. Determination of respiratory chain enzyme activities

A biochemical assay for respiratory chain enzyme activities was performed as already reported [45].

2.6. Malondialdehyde analysis

Hepatic malondialdehyde (MDA) was determined using a fluorimetric assay, based on the reaction between MDA and thiobarbituric acid [46].

2.7. Carbonylated proteins

Protein extracts were prepared to perform the analysis of hepatic carbonylated proteins. Briefly, proteins were precipitated with 200 μl chilled 20% trichloroacetic acid. Protein pellets were subsequently washed and vortexed twice with 1 ml 10% trichloroacetic acid, twice with 1 ml deionized water and once with 0.5 ml ethanol. Washing steps were performed by centrifugation at 8,000×*g* for 5 min at 4°C. The pellets were dried and dissolved in ethanol/ethyl acetate (1:1). Samples were then resuspended in protein solubilization solution and maintained for 15 min at 37°C. Carbonyl content was determined by 375 nm absorbance.

2.8. High-performance liquid chromatography of GSH

The cells were sonicated three times for 2 s in 0.1 ml of 0.1 M potassium phosphate buffer (pH 7.2). After sonication (Sonics Vibra Cell; Sonics & Material Inc., Newtown, CT, USA), the levels of total GSH, reduced GSH, oxidized (GSSG) and protein-bound (ProSSG) GSH were analyzed by high-performance liquid chromatography (HPLC). HPLC equipment and conditions for analyzing various forms of GSH have already been reported [47].

2.9. Immunoprecipitation and Western blotting

Immunoprecipitation was performed as already described [48]. Briefly, cell extracts were prepared in ice-cold RIPA lysis buffer containing 50 mM Tris, pH 7.5, 150 mM NaCl, 1% Triton X-100, 1 mM EGTA, 1% sodium deoxycholate, and 10% cocktail protease inhibitors. One hundred micrograms of proteins was immunoprecipitated overnight at 4 °C with 1 μg of anti-PTEN antibody or to nonspecific immunoglobulin G as a control. Fifteen microliters of the resuspended volume of protein A/G PLUS-agarose (Santa Cruz Biotechnology, Santa Cruz, CA, USA) was added to the solution and then incubated at 4°C for 1 h on a rocker platform. Bound fractions of precipitates and negative control were subjected to sodium dodecyl sulfate-polyacrylamide gel electrophoresis (SDS-PAGE), and blotting was performed on PVDF (polyvinylidine fluoride) membranes (Amersham, Germany). Briefly, equivalent amounts of protein were resolved on SDS-PAGE, transferred and immobilized on PVDF membranes, blocked with 5% nonfat dried milk and probed with appropriate primary and secondary antibodies (see supplementary data, Table ST1). Immunoblots were visualized with the ECL system by Amersham.

2.10. Measurement of PTEN activity

PTEN activities were measured using the PTEN Malachite Green–based phosphatase assay according to the protocol of the manufacturer (Upstate Biotechnology Inc., Lake Placid, NY, USA).

2.11. Colocalization analysis by fluorescence microscopy

Colocalization between PTEN and ProSSG was assessed by confocal microscopy using an Olympus fluoview FV1000 confocal microscope equipped with FV10-ASW version 1.6 software, multiline argon (T=458–488 and 514 nm) and 2× helium/neon (T=543 and 633 nm) lasers with 60×, 1.42-N.A. oil immersion lens. Hepatocytes were fixed with 3% paraformaldehyde (15 min at 37°C) and permeabilized with methanol for 5 min at −20°C. Primary antibodies (see additional Table ST1) were incubated overnight, followed by a 1-h incubation with secondary antibodies (Alexa). Colocalization analysis for dual-stained samples was carried out using the FV10-ASW colocalization function, and images were finally processed with Adobe Photoshop 9.0. Pearson r correlation coefficient for fluorescence intensity values was calculated for confocal channels, and percentage of colocalization was reported.

2.12. Statistical analysis

All results were expressed as means±S.D. for at least four independent experiments. Body and biochemical data were analyzed by one-way analysis of variance with repeated measures followed by post hoc least significant difference tests. Statistical differences in Western blotting were determined by Student's t test. $P<.05$ was considered statistically significant.

3. Results

3.1. Body and metabolic variables in relation to diet

As shown in Table 1, at the end of 14 weeks of diverse dietetic regimens, different patterns of body and metabolic alterations were induced. Interestingly, at the end of the experimental protocol, rats consuming HFD-LC, NFD-HF and HFD-HF gained more body weight than those consuming the SD. However, there was no difference in body weight among the groups being fed special diets. Furthermore, rats treated with HFD-LC, NFD-HF or HFD-HF showed the same significant increase of liver weight in comparison with the control group (SD).

Plasma concentrations of ALT, triglycerides, total cholesterol, glucose and insulin were also evaluated and reported in Table 1. ALT and triglyceride levels were profoundly influenced by diet; in particular, it is evident that the high-fat diet (HFD-LC or HFD-HF) induced a greater increase of ALT and triglyceride content. Total cholesterol levels were not significantly affected by the different dietetic regimens.

There was no significant difference in plasma glucose levels, and although plasma insulin concentrations tended to be very high in animals fed high-fructose diets (NFD-HF or HFD-HF), also the treatment with the only high-fat-diet (HFD-LC) significantly increased insulin compared with the controls (SD). Accordingly, the insulin trend HOMA-IR, as an insulin resistance index, was significantly increased by all hypercaloric diets (Table 1).

3.2. Food-dependent alterations of liver tissue histology and primary hepatocyte cytomorphology

As revealed by staining with H&E (Fig. 1), we found histological changes in the livers of rats fed with the different dietetic regimens compared with SD livers, which had no marked abnormalities. The HFD-LC group (Fig. 1B) presented a mild steatosis, predominantly macrovacuolar, while the NFD-HF group was essentially characterized by ballooning in numerous hepatocytes (Fig. 1C). The combination of high-fat diet with an excess fructose intake (HFD-HF) provoked ballooning associated with a rare microvacuolar and macrovacuolar steatosis (Fig. 1D).

Moreover, interestingly, the analysis with Masson's trichrome staining showed that the livers of SD, HFD-LC and NFD-HF groups were histologically normal (Fig. 1E, F and G), whereas a sporadic perisinusoidal and pericellular fibrosis emerged in liver tissues from HFD-HF rats (Fig. 1H). Interestingly, the accumulation of fat in the livers of HFD-LC and HFD-HF rats was also evident through analysis of Oil Red O staining and of intrahepatic triglyceride content (Fig. 2A–E). As demonstrated by immunohistochemical evaluation of CD45 (pan-leukocyte marker) and C163 (marker of activated Kupffer cells), infrequent inflammatory infiltrates were found only in HFD-HF rats (Fig. 2F).

Fresh primary hepatocytes, isolated from livers from each treatment group, were seeded on collagen-coated plates. The hepatocytes soon attached to the culture plates and after 1 h of culture, the hepatocytes showed the typical, uniform polygonal morphology (data not shown). Twenty-four hours later, the morphology of rat hepatocytes was analyzed using a phase-contrast microscope (Fig. 3). The majority of SD-derived hepatocytes reconstructed

Table 1
Body measurements and metabolic variables in rats at end of experiment

Variable	SD group, n=6	HFD-LC group, n=6	NFD-HF group, n=6	HFD-HF group, n=6
Body weight (g)	347.5±16.5	392.5±20.0***	396.0±22.5***	401.0±23.5***
Liver weight (g)	13.0±1.4	16.3±1.3**	16.0±1.7**	16.3±1.8**
ALT (U/l)	27.5±3.3	73.4±5.9*	29.6±4.1	75.9±8.7*
Triglycerides (mg/dl)	39.2±4.1	68.2±5.5*	46.7±3.2	89.9±7.2*
Total cholesterol (mg/dl)	0.40±0.09	0.41±0.10	0.43±0.08	0.39±0.11
Glucose (mg/dl)	73.2±7.9	85.7±7.5	78.3±8.4	93.3±8.9
Insulin (ng/ml)	0.23±0.05	0.47±0.07**	3.02±0.23*	3.54±0.28*
HOMA-IR	1.04±0.12	2.43±0.29*	14.15±1.2*	20.30±2.9*

Values are means±SD; n, number of rats.
* P<.001; **P<.01; ***P=.05 vs. SD group.

their cellular polarity presenting a typical polygonal shape, while cytomorphology of primary hepatocytes, isolated from HFD-LC, NFD-HF or HFD-HF rats, was greatly different from SD hepatocytes, which showed a more detached oval morphology (Fig. 3A–D).

3.3. Effects of dietetic regimens on primary hepatocyte homeostasis

We next examined the effects of different dietetic regimens on primary hepatocyte homeostasis. Cell homeostasis was evaluated by the analysis of cell viability, rate of DNA synthesis and mitochondrial function.

Cell viability was measured by the use of a simple vital stain, Neutral red, which provides a measure of cell activity. Primary hepatocytes isolated from rats treated with fructose-enriched diets (NFD-HF and HFD-HF) showed reduced cell viability after 24 h of culture compared with SD- and HFD-LC-derived hepatocytes (Fig. 4A). In concordance with these findings, hepatocytes from NFD-HF and HFD-HF rats showed a rate of DNA synthesis (assessed by thymidine incorporation assay), which was significantly lower than hepatocytes isolated from animals fed normal chow or a solely high-fat diet (Fig. 4B).

Altogether, these findings indicate that excessive fructose consumption may profoundly alter homeostasis of hepatocytes.

Next, we examined the effect of different diets on mitochondrial metabolism by measuring the activities of two important enzymes of the oxidative phosphorylation system in mammalian: the nicotinamide adenine dinucleotide–quinone oxidoreductase (also called complex I) and cytochrome *c* oxidase (also called complex IV). In particular, the complex I removes electrons from nicotinamide adenine dinucleotide and then transports the electrons to coenzyme Q, while the complex IV catalyzes the final reaction of the respiratory chain and functions as the final electron donor to molecular oxygen [49]. The complex I and IV activities were measured in whole-cell extracts of freshly isolated hepatocytes from animals with previously described nutritional conditions and were corrected for activity of citrate synthase representing a marker of mitochondrial number and integrity.

Interestingly, as shown in Fig. 4C, analysis of the ratio between the activities of complexes I or IV and citrate synthase activity showed that different diets did not affect the mitochondrial function of freshly isolated hepatocytes.

3.4. Markers of oxidative stress in primary hepatocytes from rats fed different diets

As markers of oxidative stress, the following indicators were measured: levels of MDA (a lipoperoxidation marker), extent of protein carbonylation (an index to evaluate protein oxidation) and, finally, levels of different forms of GSH (markers of redox status) [50]. All these markers were measured in freshly isolated primary hepatocytes from the different nutritional models described above.

As shown in Fig. 5A, there were no significant changes in MDA production among the different nutritional models. Also, the analysis of carbonylated protein levels in isolated hepatocytes showed no differences in relation to the nutritional status of the animal (Fig. 5B).

Glutathione is a tripeptide that exists in a reduced and protein-bound GSH form. Oxidized GSH may also occur as ProSSG [47]. Although reduced GSH is the active form, ratio GSSG/GSH is the most important factor in maintaining the cellular functions of GSH, especially in the liver (i.e., control of redox status and detoxification) [51,52]. Thus, we examined by HPLC the different forms of GSH in hepatocyte samples. As shown in Fig. 5C, the ratio between oxidized and reduced GSH (GSSG/GSH), and the ratio between ProSSG and total GSH (Tot GSH=GSSG+GSH+ProSSG) were significantly increased in HFD-LC, NFD-HF and HFD-HF hepatocytes compared with SD cells.

3.5. Effects of dietetic regimens on activity and posttranslational modifications of PTEN

The increased levels of glutathionylation in response to different hypercaloric regimens led us to investigate whether PTEN could be a

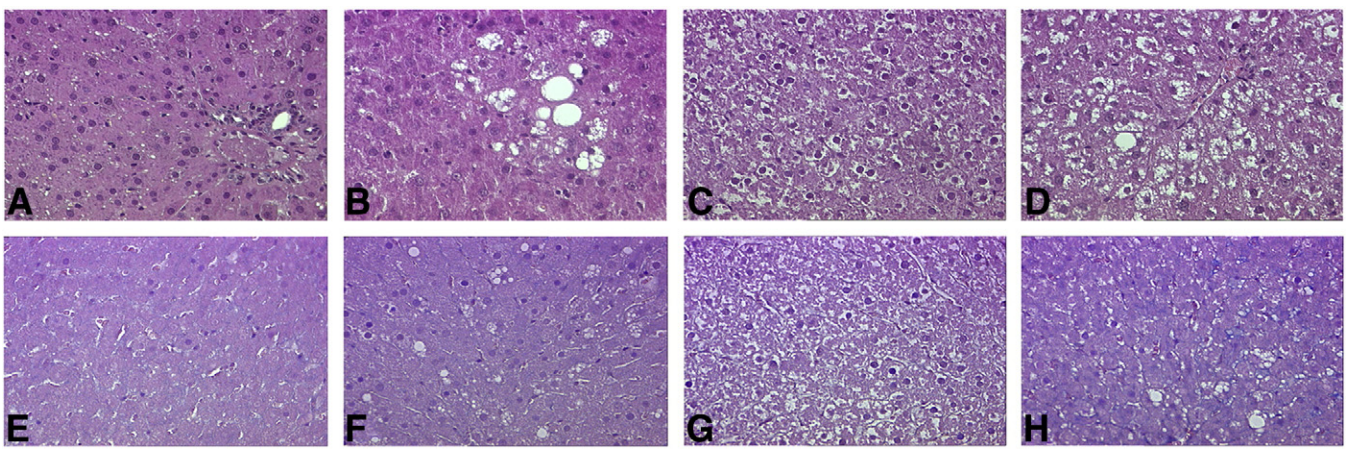

Fig. 1. Morphological changes in liver tissues from rats fed different diets. H&E staining (400×) of liver sections of SD (A), HFD-LC (B), NDF-HF (C) and HDF-HF (D) rats. Masson's trichrome staining (400×) of liver sections of SD (E), HFD-LC (F), NDF-HF (G) and HDF-HF (H) rats.

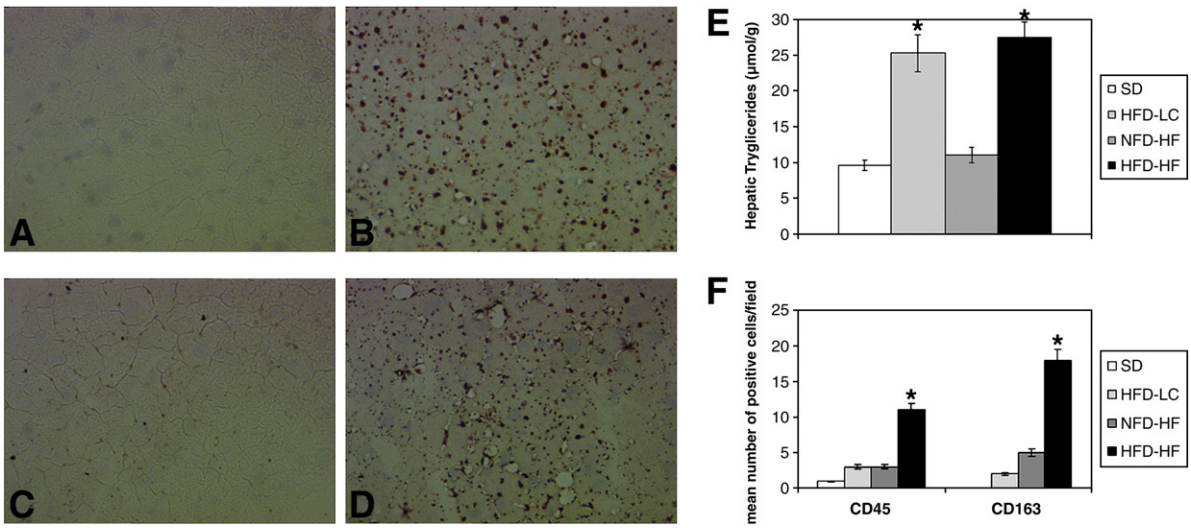

Fig. 2. Fatty changes in liver tissue from rats fed different diets. Oil Red O staining (400´) of frozen liver sections of SD (A), HFD-LC (B), NDF-HF (C) and HDF-HF (D) rats. Triglyceride content (E) measured on flash-frozen in liquid nitrogen and pulverized liver sections from SD, HFD-LC, NDF-HF and HDF-HF rats. (F) Quantification of CD45- and CD163-positive cells from SD, HFD-LC, NDF-HF and HFD-HF rats. Results are presented as mean value (±S.D.; bars) of four independent experiments. *P<.001 versus SD value.

potential target of ProSSG. As suggested by several authors, PTEN expression and activity are critical for hepatic insulin sensitivity and for the development of NAFLD [53,54]. PTEN protein exists in cells in serine/threonine phosphorylated (inactive) and dephosphorylated (active) forms. The active form of PTEN hydrolyzes phosphatidylinositol (3,4,5)-trisphosphate back to phosphatidylinositol (3,4)-bisphosphate significantly decreasing Akt phosphorylation/activation [55]. Therefore, we determined the endogenous levels of total PTEN, as well as its phosphorylation status. The expression of PTEN remained unaltered with the different diets (Fig. 6A), while the rate of PTEN phosphorylation, measured by an antibody raised against phosphoPTEN Ser^{380}, significantly increased in NFD-HF animals and even more in HFD-HF rats (Fig. 6B). Consistent with the enhanced phosphorylation/inactivation of PTEN, an increased phosphorylation/activation of Akt in serine 473 and in threonine 308 was observed (Fig. 6E and F). Furthermore, enzymatic assays revealed that PTEN activity was significantly decreased in fructose-enriched diets (NFD-HF and HFD-HF rats) compared with the SD and high-fat diet (Fig. 6H).

It is well known that, in addition to its phosphorylation, PTEN activity and stability are considerably influenced by the oxidation (glutathionylation) of susceptible cysteine residues and ubiquitination of specific lysine residues [55–57]. Thus, we performed an immunoprecipitation assay to determine the interaction of endogenous PTEN with both GSH and ubiquitin. As shown in Fig. 7, PTEN was either glutathionylated or ubiquitinated (formed immunocomplexes with both ProSGG and ubiquitin). Immunoprecipitation assay (Fig. 7A) and colocalization analysis (Fig. 7B) showed that glutathionylated PTEN was significantly up-regulated in rats fed a high-fructose diet (NFD-HF and HFD-HF). On the contrary, PTEN mono-ubiquitination, as indicated by about 64-kDa molecular weight, was lower in all the animals fed hypercaloric diets compared with animals treated with a standard dietetic regimen (Fig. 7C).

4. Discussion

The main driving force for the increased prevalence of fatty liver and NASH is modern Westernized dietary habits, with their increased

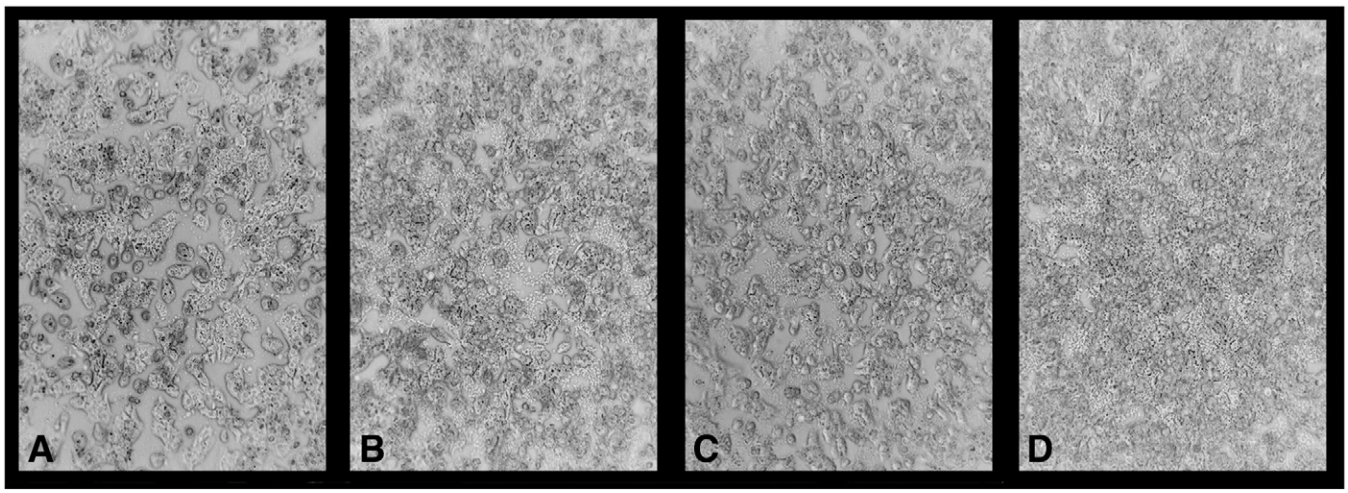

Fig. 3. Cellular morphology of primary hepatocytes isolated from rats treated with different diets. Phase-contrast photomicrographs (400×) showing cellular morphology of primary hepatocytes isolated from rats treated with (A) SD, (B) HFD-LC, (C) NFD-HF and (D) HFD-HF after 24 h of culture.

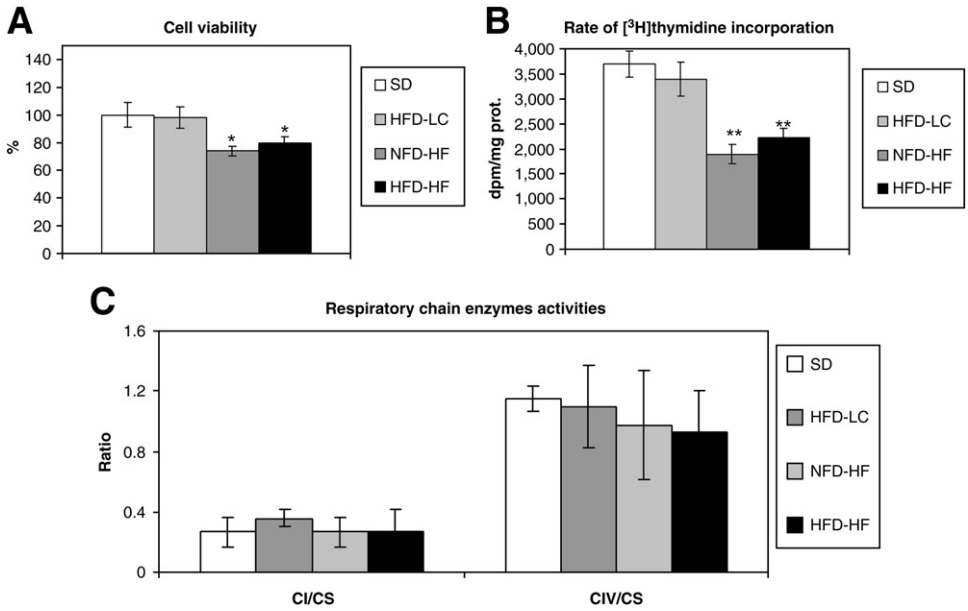

Fig. 4. Cell viability, DNA synthesis and respiratory chain enzyme activities of primary hepatocytes from rats treated with different diets. (A) Cell viability at 24 h was evaluated by a neutral red assay and reported as percentage compared with the control (SD). (B) DNA synthesis was evaluated as [^{3}H]thymidine incorporations after 24 h from seeding. Quantitative data were reported as dpm/mg prot. (C) Ratio between the activities of complexes I or IV and citrate synthase activity (CS) was calculated in whole-cell extracts of freshly isolated hepatocytes. Histograms are the mean value (±S.D.; bars) of four independent experiments. *P<.001; **P<.01 versus SD value.

caloric intake, and eating patterns, which increase the risk of obesity [22]. Several rodent models have been used to study the pathogenesis of NAFLD [58]. In view of the multifactorial etiology of this disease, the most commonly used models, based on genetic manipulation (e.g., *ob*/*ob* mouse) or on toxic injury (e.g., methionine–choline-deficient diet), often may not reflect the real metabolic context of developing human disease and may fail to reproduce the whole spectrum of liver pathology that characterizes human NAFLD [59,60]. Actually, models of chronic overnutrition with spontaneous progression of steatosis to steatohepatitis may be the most valid and practical means for understanding the pathophysiology of this condition [58].

The model used in this study mimics well all typical Westernized diets, which consist mostly of increased carbohydrate and/or fat intake. According to the literature, our results indicate that both high-fat and high-fructose regimens may alter body characteristics and metabolic variables in rats [61]. Our data essentially demonstrate that although weight gain is similar in all hypercaloric diets, metabolic disturbances (i.e., altered levels of ALT, triglycerides and insulin) are exacerbated by the presence of an elevated dietary intake of fructose either alone or in combination with high fats. It is noteworthy that composition of diets is relevant for determining liver tissue damage. In fact, animals fed a fructose-enriched diet present only diffuse ballooning degeneration in hepatocyte cytoplasm, while

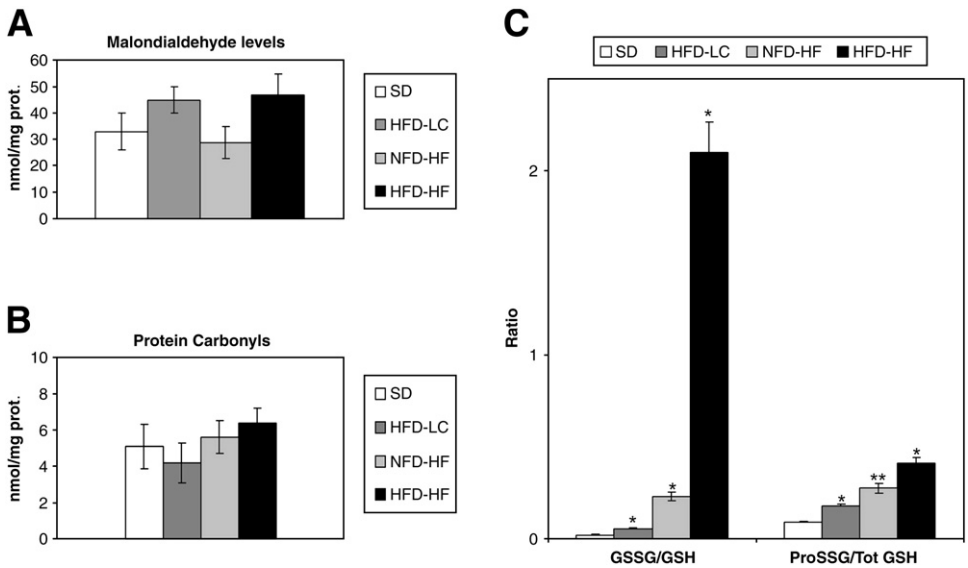

Fig. 5. Levels of MDA, carbonylated proteins and different forms of GSH in primary hepatocytes from rats treated with different diets. (A) MDA levels were measured in whole-cell extracts of freshly isolated hepatocytes. Quantitative data were reported as nmol/mg prot. (B) Protein carbonyls of fresh hepatocytes were reported as mol/mg prot. (C) HPLC analysis of different GSH forms. The GSSG/GSH and ProSSG/Tot GSH ratios were reported. Histograms are the mean value (±S.D.; bars) of four independent experiments. *P<.001; **P<.01 versus SD value.

liver tissue of high-fat rats are characterized by a rare microsteatosis and macrosteatosis, and the combination of the two dietetic regimens results in a mishmash of both liver features. Consistent with the data of Kawasaki et al. [62], our findings highlight that rats fed fructose-enriched diets resemble NASH more than rats fed high-fat diets.

In this framework, oxidative stress might also play a different role, both in promoting and/or worsening the molecular and structural hepatic abnormalities accompanying diet-associated liver disease. Our results demonstrated that excessive fructose intake reduces viability and proliferation of hepatocytes and disturbs their redox equilibrium, high-fat diet affects only redox status and, finally, the impairment of hepatocyte homeostasis due to a high-fat diet enriched with fructose is a sum of both effects.

Interestingly, levels of ProSSG seem to be more likely to increase in hypercaloric diets. These findings confirm our previous in vitro data that emphasize enhanced glutathionylation in liver tissue from children with NAFLD [40]. Interestingly, here we found changes of balance between GSSG and GSH in the absence of mitochondrial dysfunction. Although further studies are required to assess the exact mechanism, we believe that the alterations of redox homeostasis may depend on the network of interactions between fructose/reactive oxygen species and toll-like receptor 4, which in turn control nuclear transcription factors potentially involved in the regulation of GSH S-transferase transcription, GSH synthesis, or alternatively, in the regulation of GSH hepatic transport [63,64].

Protein glutathionylation plays a critical role in regulating the activity and stability of several different proteins, including PTEN [56,65]. PTEN deficiency induces numerous cellular injuries via the activation of Akt signaling, but it was also shown that PTEN deficiency in hepatocytes is able to induce hepatic steatosis, inflammation and fibrosis resembling NAFLD/NASH [41]. Moreover, results from a recent study suggest that PTEN/Akt/lipids networks control hepatic lipid metabolism in different ways that might be related to the source of lipids (i.e., genetic induced visceral fat accumulation or diet intake) [66]. These findings suggest that PTEN is a key protein in determining molecular derangement that occurs during NAFLD development, but no data on hepatic PTEN expression pattern and activity in a model of dietetic NAFLD have been reported to date. In this study, we demonstrated that high-fructose intake causes, in hepatocytes, an increased serine phosphorylation of PTEN, which is consistent with the inhibition of its phosphatase activity. Activity of PTEN shows an antiparallel trend with respect to its glutathionylation and tends to a positive correspondence with the mono-ubiquitination of protein. The biochemical interplay between PTEN activity, phosphorylation, glutathionylation and ubiquitination is still obscure and requires further biochemical investigation. However, we have formulated a hypothesis, based on literature [67,68], our results and a prediction model of the glutathionylated and ubiquitinated residues of PTEN (Supplementary Figure 1, SF1). A high-fructose diet, via redox homeostasis imbalance, might induce PTEN glutathionylation in the phosphatase domain, to make the protein more prone to phosphorylation and consequent inactivation. Reduced PTEN mono-ubiquitination, as suggested by other authors, might be an indicator of cytoplasmic retention rather than a signal of degradation; in fact, parallel to decreased PTEN mono-ubiquitination, we observed decreased nuclear levels of PTEN (Supplementary Figure 2, SF2)[57].

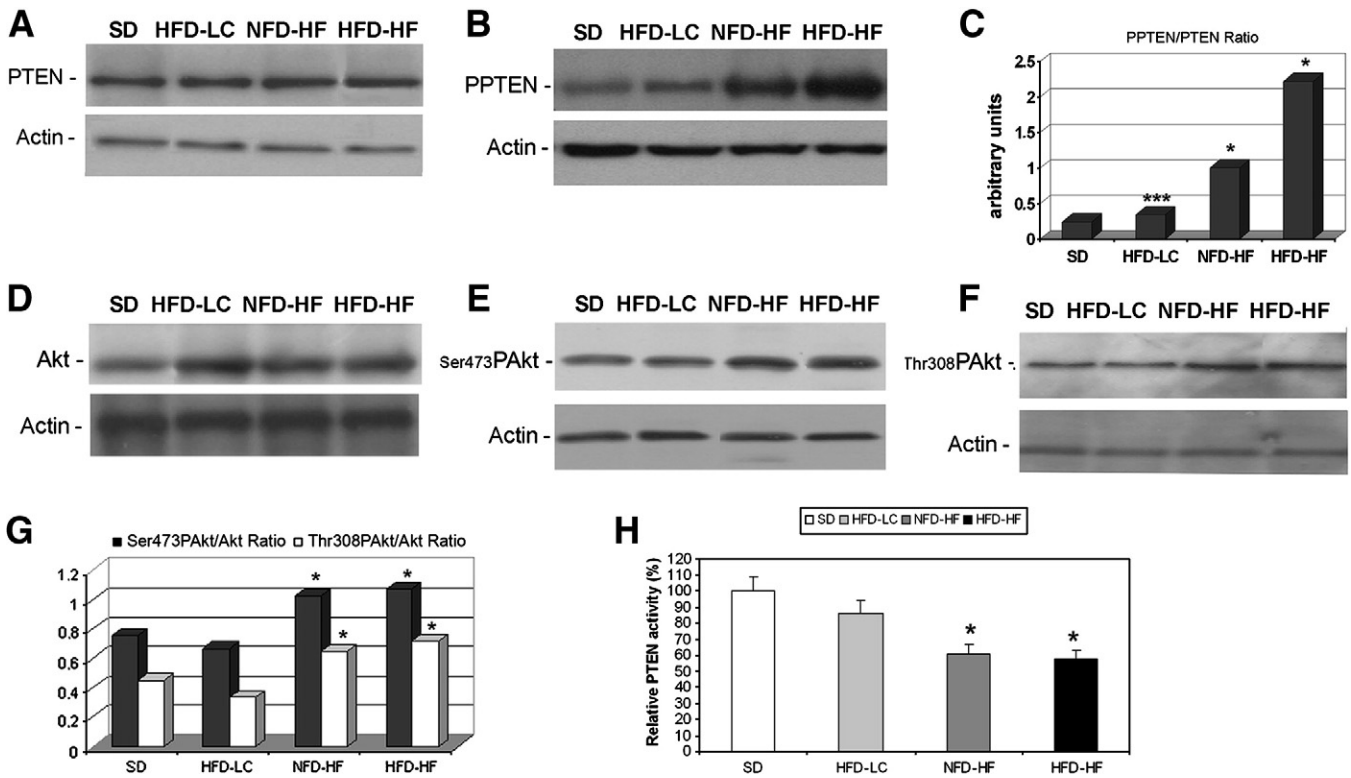

Fig. 6. Expression and activity of PTEN in primary hepatocytes freshly from rats treated with different diets. Levels of total PTEN (A) and serine-phosphorylated PTEN (B) were assayed by immunoblotting with specific antibodies (upper panels). Levels of β-actin (lower panels) were reported as equal loading control. (C) Ratio between phosphorylated PTEN and total PTEN was reported. Levels of total Akt (D), serine 473 Akt (E) and threonine 308 phosphorylated Akt (F). (G) Ratio between densitometric quantification of phosphorylated forms of Akt and total Akt was reported. Representative gels from one of five separate experiments are shown. (H) PTEN activity was measured with quantitative phosphatase assay in isolated hepatocytes. Histograms reported data of five independent experiments (±S.D.; bars). *P<.001; ***P<.05 versus SD value.

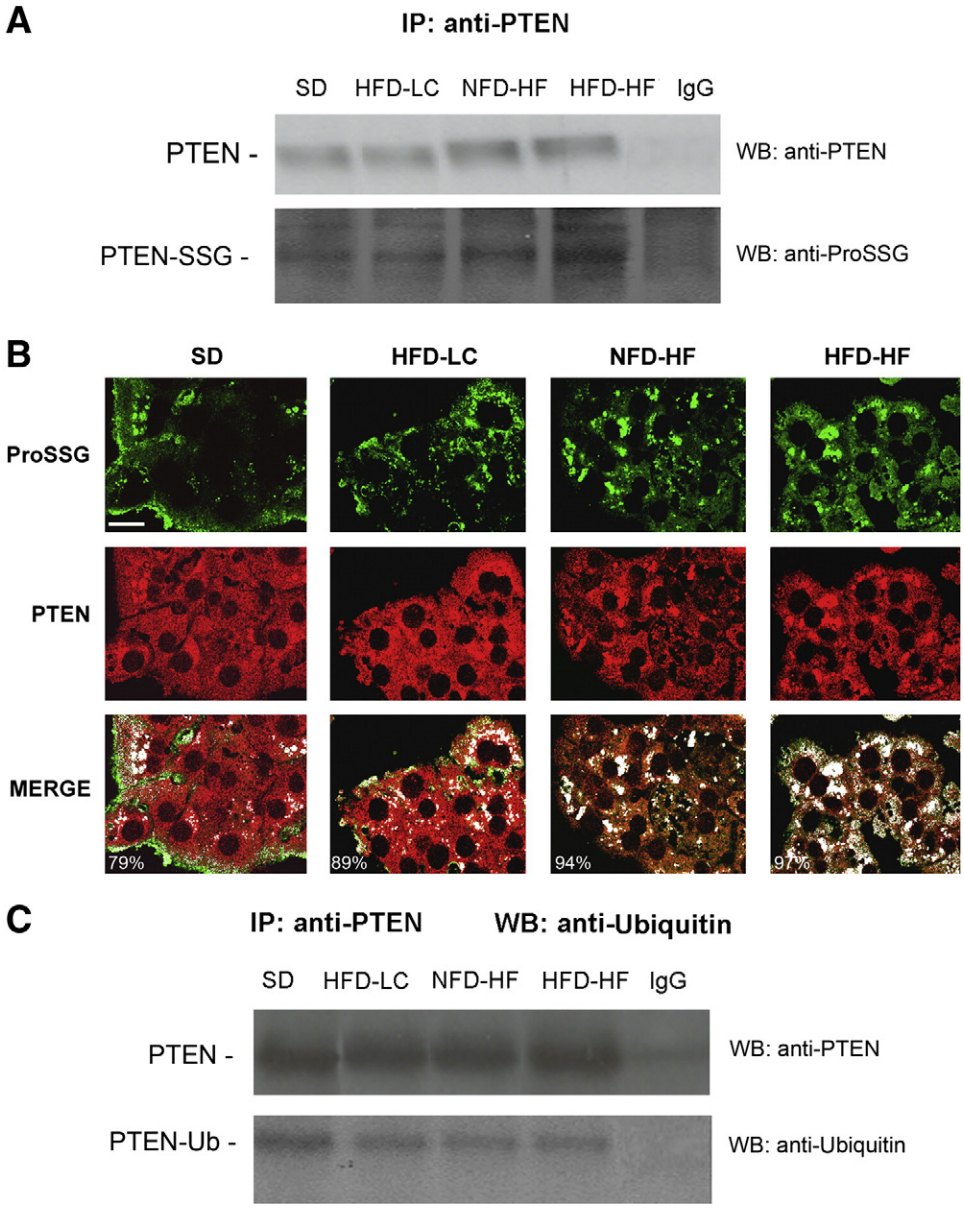

Fig. 7. PTEN glutathionylation and ubiquitination in primary hepatocytes from rats treated with different diets. Cells were lysed and subjected to immunoprecipitation with anti-PTEN antibody or a control immunoprecipitation using equivalent amounts of nonspecific rabbit antimouse immunoglobulin G. The immunocomplexes were separated by SDS-PAGE under nonreducing conditions and immunoblotted with anti-PTEN or anti-ProSSG (A). A representative gel from one of four separate experiments is shown. (B) Representative confocal immunofluorescences using anti-ProSSG antibody (green) anti-PTEN antibody (red) are shown. Merge images (green–red) and colocalization points (white) are showed in the same panels. Values in the colocalization panel indicate percentage of colocalization. Magnification bar: 30 μm. (C) A representative immunoblotting with anti-PTEN or anti-ubiquitin antibody from one of four independent experiments is shown.

The mechanism that connects fructose and PTEN increased phosphorylation/inactivation remains unclear. However, we found that glycogen synthase kinase 3β (GSK3β), one of kinases potentially involved in PTEN regulation, is significantly activated/dephosphorylated in fructose-enriched diets (Supplementary Figure 2, SF3) [69]. As predicted by MINT (a Molecular INTeraction database, http://mint.bio.uniroma2.it/mint/Welcome.do), GSK3β might physically and functionally interacts with a protein that was found already up-regulated by fructose: the protein-tyrosine phosphatase 1B [70]. Further studies are needed to verify this hypothesis.

In conclusion, we believe that two elements constitute the novelty and originality of this study. First, our results suggest that, since the measurement of oxidative stress markers in plasma does not always reproduce hepatic oxidative damage, it is preferable to study this phenomenon directly on hepatic cells. Second, we have demonstrated that excessive fructose intake causes different tissue damage compared with the high-fat diet alone and makes the hepatocytes more prone to posttranslational modifications and activity alteration of PTEN.

Supplementary materials related to this article can be found online at doi:10.1016/j.jnutbio.2010.11.013.

Acknowledgments

We thank Marco Pezzullo for his technical contribution to the liver histology.

References

[1] Lau C, Fearch K, Glumer C, Tetens I, Pedersen O, Carstensen B, et al. Inter99 study. Dietary glycemic index, glycemic load, fiber, simple sugar, and insulin resistance. Diabetes Care 2005;28:1397–403.
[2] Hine RJ. Time to get specific about dietary carbohydrates, affected populations, and diseases. Am J Clin Nutr 2008;87:1062.
[3] Vilar L, Oliveira CP, Faintuch J, Mello ES, Nogueira MA, Santos TE, et al. High-fat diet: a trigger of non-alcoholic steatohepatitis? Preliminary findings in obese subjects. Nutrition 2008;24:1097–102.
[4] Leite ML, Nicolosi A. Dietary patterns and metabolic syndrome factors in a non-diabetic Italian population. Public Health Nutr 2009;15:1–10.
[5] Drewnowski A. The real contribution of added sugars and fats to obesity. Epidemiol Rev 2007;29:160–71.
[6] Astrup A, Dyerberg J, Selleck M, Stender S. Nutrition transition and its relationship to the development of obesity and related chronic diseases. Obes Rev 2008;9 (Suppl 1):48–52.
[7] van Baak MA, Astrup A. Consumption of sugars and body weight. Obes Rev 2009;10(Suppl 1):9–23.
[8] Sherwood NE, Jeffery RW, French SA, Hannan PJ, Murray DM. Predictors of weight gain in the Pound of Prevention study. Int J Obes Relat Metab Disord 2000;24: 395–403.
[9] Storlien LH, Higgins JA, Thomas TC, Brown MA, Wang HQ, Huang XF, et al. Diet composition and insulin action in animal models. Br J Nutr 2000;83(Suppl 1): 85–90.
[10] Woods SC, D'Alessio DA, Tso P, Rushing PA, Clegg DJ, Benoit SC, et al. Consumption of a high-fat diet alters the homeostatic regulation of energy balance. Physiol Behav 2004;83:573–8.
[11] Buettner R, Schölmerich J, Bollheimer LC. High-fat diets: modeling the metabolic disorders of human obesity in rodents. Obesity (Silver Spring) 2007;15:798–808.
[12] Willet WC. Overview and perspective in human nutrition. Asia Pac J Clin Nutr 2008;17(Suppl 1):1–4.
[13] Elahi MM, Cagampang FR, Mukhtar D, Anthony FW, Ohri SK, Hanson MA. Long-term maternal high-fat feeding from weaning through pregnancy and lactation predisposes offspring to hypertension, raised plasma lipids and fatty liver in mice. Br J Nutr 2009;10:1–6.
[14] Gaesser GA. Carbohydrate quantity and quality in relation to body mass index. J Am Diet Assoc 2007;107:1768–80.
[15] van Dam RM, Seidell JC. Carbohydrate intake and obesity. Eur J Clin Nutr 2007;61 (Suppl 1):75–99.
[16] Stanhope KL, Havel PJ. Endocrine and metabolic effects of consuming beverages sweetened with fructose, glucose, sucrose, or high-fructose corn syrup. Am J Clin Nutr 2008;88:1733S–7S.
[17] Johnson RJ, Segal MS, Sautin Y, Nakagawa T, Feig DI, Kang DH, et al. Potential role of sugar (fructose) in the epidemic of hypertension, obesity and the metabolic syndrome, diabetes, kidney disease, and cardiovascular disease. Am J Clin Nutr 2007;86:899–906.
[18] Bray GA. Fructose: should we worry? Int J Obes (Lond) 2008;32(Suppl 7):127–31.
[19] Miller A, Adeli K. Dietary fructose and the metabolic syndrome. Curr Opin Gastroenterol 2008;24:204–9.
[20] Stanhope KL, Schwarz JM, Keim NL, Griffen SC, Bremer AA, Graham JL, et al. Consuming fructose-sweetened, not glucose-sweetened, beverages increases visceral adiposity and lipids and decreases insulin sensitivity in overweight/obese humans. J Clin Invest 2009;119:1322–34.
[21] Abdelmalek MF, Suzuki A, Guy C, Unalp-Arida A, Colvin R, Johnson RJ, et al. Nonalcoholic Steatohepatitis Clinical Research Network. Increased fructose consumption is associated with fibrosis severity in patients with nonalcoholic fatty liver disease. Hepatology 2010;51:1961–71.
[22] Cave M, Deaciuc I, Mendez C, Song Z, Joshi-Barve S, Barve S, et al. Nonalcoholic fatty liver disease: predisposing factors and the role of nutrition. J Nutr Biochem 2007;18:184–95.
[23] Tetri LH, Basaranoglu M, Brunt EM, Yerian LM, Neuschwander-Tetri BA. Severe NAFLD with hepatic necroinflammatory changes in mice fed trans fats and a high-fructose corn syrup equivalent. Am J Physiol Gastrointest Liver Physiol 2008;295: G987–95.
[24] Basciano H, Miller AE, Naples M, Baker C, Kohen R, Xu E, et al. Metabolic effects of dietary cholesterol in an animal model of insulin resistance and hepatic steatosis. Am J Physiol Endocrinol Metab 2009;297:E462–73.
[25] Bondini, S., Kleiner, D.E., Goodman, Z.D., Gramlich, T., Younossi, Z.M., Pathologic assessment of non-alcoholic fatty liver disease. Clin Liver Dis. 2007;11: 17-23, vii.
[26] Paradis V, Bedossa P. Definition and natural history of metabolic steatosis: histology and cellular aspects. Diabetes Metab 2008;34:638–42.
[27] Wilfred de Alwis NM, Day CP. Genetics of alcoholic liver disease and nonalcoholic fatty liver disease. Semin Liver Dis 2007;27:44–54.
[28] Alisi A, Manco M, Vania A, Nobili V. Pediatric nonalcoholic fatty liver disease in 2009. J Pediatr 2009;155:469–74.
[29] Romestaing C, Piquet MA, Bedu E, Rouleau V, Dautresme M, Hourmand-Ollivier I, et al. Long term highly saturated fat diet does not induce NASH in Wistar rats. Nutr Metab 2007;4:4.
[30] Lieber CS, Leo MA, Mak KM, Xu Y, Cao Q, Ren C, et al. Model of non-alcoholic steatohepatitis. Am J Clin Nutr 2004;79:502–9.
[31] Svegliati-Baroni G, Candelaresi C, Saccomanno S Ferretti G, Bachetti T, Marzioni M, De Minicis S, et al. A model of insulin resistance and nonalcoholic steatohepatitis in rats: role of peroxisome proliferator-activated receptor-alpha and n-3 polyunsaturated fatty acid treatment on liver injury. Am J Pathol 2006;169: 846–60.
[32] Surwit R, Feinglos M, Rodin J, Sutherland A, Petro A, Opara E, et al. Differential effects of fat and sucrose on the development of obesity and diabetes in C57BL/6J and A/J mice. Metabolism 1995;44:645–51.
[33] MacQueen HA, Sadler DA, Moore SA, Daya S, Brown JY, Shuker DEG, et al. Deleterious effects of a cafeteria diet on the livers of nonobese rats. Nutr Res 2007;27:38–47.
[34] Pessayre D. Role of mitochondria in non-alcoholic fatty liver disease. J Gastroenterol Hepatol 2007;22(Suppl 1):20–7.
[35] Malaguarnera M, Di Rosa M, Nicoletti F, Malaguarnera L. Molecular mechanisms involved in NAFLD progression. J Mol Med 2009;87:679–95.
[36] Tessari P, Coracina A, Cosma A, Tiengo A. Hepatic lipid metabolism and non-alcoholic fatty liver disease. Nutr Metab Cardiovasc Dis 2009;19:291–302.
[37] Mantena SK, Vaughn DP, Andringa KK, Eccleston HB, King AL, Abrams GA, et al. High fat diet induces dysregulation of hepatic oxygen gradients and mitochondrial function in vivo. Biochem J 2009;417:183–93.
[38] Feillet-Coudray C, Sutra T, Fouret G, Ramos J, Wrutniak-Cabello C, Cabello G, et al. Oxidative stress in rats fed a high-fat high-sucrose diet and preventive effect of polyphenols: involvement of mitochondrial and NAD(P)H oxidase systems. Free Radic Biol Med 2009;46:624–32.
[39] Machado MV, Ravasco P, Jesus L, Marques-Vidal P, Oliveira CR, Proença T, et al. Blood oxidative stress markers in non-alcoholic steatohepatitis and how it correlates with diet. Scand J Gastroenterol 2008;43:95–102.
[40] Piemonte F, Petrini S, Gaeta LM, Tozzi G, Bertini E, Devito R, et al. Protein glutathionylation increases in the liver of patients with non-alcoholic fatty liver disease. J Gastroenterol Hepatol 2008;23:457–64.
[41] Watanabe S, Horie Y, Kataoka E, Dohmen T, Ohshima S, Goto T, et al. Non-alcoholic steatohepatitis and hepatocellular carcinoma: lessons from hepatocyte-specific phosphatase and tensin homolog (PTEN)-deficient mice. J Gastroenterol Hepatol 2007;22(Suppl 1):96–100.
[42] Leoni S, Spagnuolo S, Massimi M, Terenzi F, Conti Devirgiliis L. Amino acid uptake regulation by cell growth in cultured hepatocytes isolated from fetal and adult rats. Biosci Rep 1992;12:135H–41H.
[43] Babich H, Borenfreund E. Cytotoxicity of T-2 toxin and its metabolites determined with the neutral red cell viability assay. Appl Environ Microbiol 1991;57:2101–3.
[44] Alisi A, Spagnuolo S, Napoletano S, Spaziani A, Leoni S. Thyroid hormones regulate DNA-synthesis and cell-cycle proteins by activation of PKCalpha and p42/44 MAPK in chick embryo hepatocytes. J Cell Physiol 2004;201:259–65.
[45] Piemonte F, Casali C, Carrozzo R, Schägger H, Patrono C, Tessa A, et al. Respiratory chain defects in hereditary spastic paraplegias. Neuromuscul Disord 2001;11: 565–9.
[46] Conti M, Morand PC, Levillain P, Lemonnier A. Improved fluorometric determination of malonaldehyde. Clin Chem 1991;37:1273–5.
[47] Pastore A, Federici G, Bertini E, Piemonte F. Analysis of glutathione: implication in redox and detoxification. Clin Chim Acta 2003;333:19–39.
[48] Alisi A, Piemonte F, Pastore A, Panera N, Passarelli C, Tozzi G, et al. Glutathionylation of p65NF-kappaB correlates with proliferating/apoptotic hepatoma cells exposed to pro- and anti-oxidants. Int J Mol Med 2009;24: 319–26.
[49] Fernández-Vizarra E, Tiranti V, Zeviani M. Assembly of the oxidative phosphorylation system in humans: what we have learned by studying its defects. Biochim Biophys Acta 2009;1793:200–11.
[50] Valko M, Leibfritz D, Moncol J, Cronin MT, Mazur M, Telser J. Free radicals and antioxidants in normal physiological functions and human disease. Int J Biochem Cell Biol 2007;39:44–84.
[51] Han D, Hanawa N, Saberi B, Kaplowitz N. Mechanisms of liver injury. III. Role of glutathione redox status in liver injury. Am J Physiol Gastrointest Liver Physiol 2006;291:G1–7.
[52] Nobili V, Pastore A, Gaeta LM, Tozzi G, Comparcola D, Sartorelli MR, et al. Glutathione metabolism and antioxidant enzymes in patients affected by nonalcoholic steatohepatitis. Clin Chim Acta 2005;355:105–11.
[53] Vinciguerra M, Foti M. PTEN at the crossroad of metabolic diseases and cancer in the liver. Ann Hepatol 2008;7:192–9.
[54] Vinciguerra M, Veyrat-Durebex C, Moukil MA, Rubbia-Brandt L, Rohner-Jeanrenaud F, Foti M. PTEN down-regulation by unsaturated fatty acids triggers hepatic steatosis via an NF-kappaBp65/mTOR-dependent mechanism. Gastroenterology 2008;134:268–80.
[55] Leslie NR, Batty IH, Maccario H, Davidson L, Downes CP. Understanding PTEN regulation: PIP2, polarity and protein stability. Oncogene 2008;27: 5464–76.
[56] Yu CX, Li S, Whorton AR. Redox regulation of PTEN by S-nitrosothiols. Mol Pharmacol 2005;68:847–54.
[57] Trotman LC, Wang X, Alimonti A, Chen Z, Teruya-Feldstein J, Yang H, et al. Ubiquitination regulates PTEN nuclear import and tumor suppression. Cell 2007;128:141–56.
[58] Larter CZ, Yeh MM. Animal models of NASH: getting both pathology and metabolic context right. J Gastroenterol Hepatol 2007;23:1635–48.
[59] Anstee QM, Goldin RD. Mouse models in non-alcoholic fatty liver disease and steatohepatitis research. Int J Exp Pathol 2006;87:1–16.
[60] Postic C, Girard J. Contribution of de novo fatty acid synthesis to hepatic steatosis and insulin resistance: lessons from genetically engineered mice. Clin Invest 2008;118:829–38.

[61] Schaalan M, El-Abhar HS, Barakat M, El-Denshary ES. Westernized-like-diet-fed rats: effect on glucose homeostasis, lipid profile, and adipocyte hormones and their modulation by rosiglitazone and glimepiride. J Diabetes Complications 2009;23:199–208.
[62] Kawasaki T, Igarashi K, Koeda T, Sugimoto K, Nakagawa K, Hayashi S, et al. Rats fed fructose-enriched diets have characteristics of nonalcoholic hepatic steatosis. J Nutr 2009;139:2067–71.
[63] Spruss A, Kanuri G, Wagnerberger S, Haub S, Bischoff SC, Bergheim I. Toll-like receptor 4 is involved in the development of fructose-induced hepatic steatosis in mice. Hepatology 2009;50:1094–104.
[64] Su B. Linking stress to immunity? Nat Immunol 2005;6:541–2.
[65] Wang X, Jiang X. Post-translational regulation of PTEN. Oncogene 2008;27: 5454–63.
[66] Leavens KF, Easton RM, Shulman GI, Previs SF, Birnbaum MJ. Akt2 is required for hepatic lipid accumulation in models of insulin resistance. Cell Metab 2009;10: 405–18.
[67] Sanchez R, Riddle M, Woo J, Momand J. Prediction of reversibly oxidized protein cysteine thiols using protein structure properties. Protein Sci 2008;17: 473–81.
[68] Radivojac P, Vacic V, Haynes C, Cocklin RR, Mohan A, Heyen JW, et al. Identification, analysis, and prediction of protein ubiquitination sites. Proteins 2010;78:365–80.
[69] Tamguney T, Stokoe D. New insights into PTEN. J Cell Sci 2007;120:4071–9.
[70] Wei Y, Pagliassotti MJ. Hepatospecific effects of fructose on c-jun NH2-terminal kinase: implications for hepatic insulin resistance. Am J Physiol Endocrinol Metab 2004;287:E926–33.